Unravelling Glucan Recognition Systems by Glycome Microarrays Using the Designer Approach and Mass Spectrometry*⑤

Angelina S. Palma‡§***, Yan Liu‡, Hongtao Zhang‡ ‡‡‡, Yibing Zhang‡,
Barry V. McCleary¶, Guangli Yu‖, Qilin Huang**§§§, Leticia S. Guidolin‡‡,
Andres E. Ciocchini‡‡, Antonella Torosantucci§§, Denong Wang¶¶,
Ana Luísa Carvalho§, Carlos M. G. A. Fontes‖‖‖, Barbara Mulloy‡, Robert A. Childs‡,
Ten Feizi‡, and Wengang Chai‡***

Glucans are polymers of D-glucose with differing linkages in linear or branched sequences. They are constituents of microbial and plant cell-walls and involved in important bio-recognition processes, including immunomodulation, anticancer activities, pathogen virulence, and plant cell-wall biodegradation. Translational possibilities for these activities in medicine and biotechnology are considerable. High-throughput micro-methods are needed to screen proteins for recognition of specific glucan sequences as a lead to structure–function studies and their exploitation. We describe construction of a "glucome" microarray, the first sequence-defined glycome-scale microarray, using a "designer" approach from targeted ligand-bearing glucans in conjunction with a novel high-sensitivity mass spectrometric sequencing method, as a screening tool to assign glucan recognition motifs. The glucome microarray comprises 153 oligosaccharide probes with high purity, representing major sequences in glucans. Negative-ion electrospray tandem mass spectrometry with collision-induced dissociation was used for complete linkage analysis of gluco-oligosaccharides in linear "homo" and "hetero" and branched sequences. The system is validated using antibodies and carbohydrate-binding modules known to target α- or β-glucans in different biological contexts, extending knowledge on their specificities, and applied to reveal new information on glucan recognition by two signaling molecules of the immune system against pathogens: Dectin-1 and DC-SIGN. The sequencing of the glucan oligosaccharides by the MS method and their interrogation on the microarrays provides detailed information on linkage, sequence and chain length requirements of glucan-recognizing proteins, and are a sensitive means of revealing unsuspected sequences in the polysaccharides. *Molecular & Cellular Proteomics* 14: 10.1074/mcp.M115.048272, 974–988, 2015.

Glucan polysaccharides are polymers of D-glucose with differing linkages in linear or branched sequences. They occur as storage materials in animals, secreted virulence factors of bacteria, and conserved structural components of cell walls of yeasts, fungi, some bacteria, and plants. Polysaccharides of this type are of considerable interest in biology, medicine, and biotechnology and are acknowledged for their immuno-stimulatory, anticancer, and health-promoting activities (1, 2); for their elicitor activities in defense responses and signaling in plants (3); and for acting as functional ingredients in human nutrition (4). Unraveling recognition systems that mediate these activities is highly desirable as a lead to effective translational applications.

Recognition systems involving glucan polysaccharides include those in mammals, such as recognition of fungal β-glucans by Dectin-1, the major receptor of the innate immune system against fungal pathogens (5), and by natural or vaccine-induced protective antifungal antibodies (6, 7); also recognition of mycobacterial α-glucan by the innate immune

receptor DC-SIGN (dendritic cell-specific ICAM-3-grabbing nonintegrin) (8); those in insects, such as the Drosophila Gram-negative binding protein 3 (GNBP3) sensor protein, which binds β-glucans (9); and those in bacteria, such as *Brucella abortus*, where cyclic β-glucans can serve as virulence factors (10).

Another important class of glucan-recognizing proteins comprises noncatalytic carbohydrate-binding modules (CBMs)[1] of bacterial glycoside hydrolases that mediate association with substrate and increase catalytic activity, likely through a targeting mechanism or by driving enzyme specificity (11, 12). Notable examples are CBMs of bacterial cellulolytic enzymes that promote enzymatic deconstruction of intact plant cell walls and that are of industrial significance in the biofuel and bioprocessing sectors (13, 14) and CBMs of rumen or commensal human microbiota with roles in animal and human health (14, 15). CBMs also have roles in other systems: for example, CBM-containing enzymes as virulence factors of bacterial pathogens (16) and CBM-containing human laforin that regulates glycogen metabolism and for which mutations can lead to neurodegenerative disease (17). The number of putative glucan-binding CBMs that have been identified and classified in the Carbohydrate-Active enZyme (CAZy) database (http://www.cazy.org) is expanding, but relatively few have been experimentally investigated for details of carbohydrate binding and fine specificity (11).

Searching for and assigning the specificities of glucan-recognizing proteins has thus become increasingly important. It is desirable to have high-throughput and sensitive micro-methods to screen for and characterize ligands for structure–function studies toward effective exploitation in modern therapeutic, nutritional, agricultural, and biofuel-related technologies. Carbohydrate microarrays have served to advance knowledge on specificities of diverse carbohydrate-recognition systems (18–22). Where the desired oligosaccharide probes are unavailable, microarrays need to be generated from ligand-bearing glycomes (23). Using a prototype of such designer microarrays of neoglycolipid (NGL)-probes (23) derived from oligosaccharide fragments of glucans rich in β1,3- or β1,6-linked sequences, we showed that linear β1,3-linked glucose sequences with degree of polymerization (DP) 10 or longer are bound by Dectin-1 (24). Recognition of other types of glucan sequences by Dectin-1 and the applicability of microarrays of diverse gluco-oligosaccharide sequences to other glucan-recognizing proteins required investigation. Cummings, Smith, and colleagues have developed the shotgun strategy (20) to create glycome-scale "gangliome" and "human milk glycome" microarrays. In the shotgun microarrays, the printed probes may not be sequence-defined before array construction and require

metadata-assisted glycan sequencing (MAGS), which combines MS analysis (25), binding data with glycan-binding proteins or antibodies, and exoglycosidase treatment after printing (26, 27).

Mass spectrometry has become a primary technique in carbohydrate structural analysis (28), and electrospray mass spectrometry (ESI-MS) has been used to provide sequence and partial linkage information on various types of oligosaccharides (29–33). For neutral oligosaccharides, we have found that tandem MS with collision-induced dissociation (CID-MS/MS) in the negative-ion mode is particularly useful and have successfully applied for oligosaccharide chain and blood-group typing (34, 35) and for branching pattern analysis (36).

This is because that some important linkages at certain monosaccharide residues can be unambiguously determined with high sensitivity without the need for derivatization and anion complexation as previously recognized, *e.g.* in the area of gluco-oligosaccharides, Cl^--anion adduction has been used to determine sequences of tetrasaccharides of dextran (37).

Here, we describe a strategy using the designer approach combined with negative-ion ESI-CID-MS/MS for constructing a microarray of sequence-defined gluco-oligosaccharides representing major sequences in glucans (glucome microarray) as a tool for screening glucan-recognizing proteins and assigning their recognition motifs (Fig. 1). We selected a comprehensive panel of glucan polysaccharides isolated from plants, fungi, and bacteria with different sequences to represent the glucome. We used finely tuned chemical and enzymatic methods to partially depolymerize the polysaccharides and prepare gluco-oligosaccharide fragments with different chain lengths (up to DP-13 or DP-16). We developed a ESI-CID-MS/MS method that enables linkage and sequence determination of linear or branched gluco-oligosaccharides at high-sensitivity and applied this to the sequencing of oligosaccharide fragments prepared. These sequence-defined gluco-oligosaccharides were then converted into NGL probes and used for construction of the microarray. The oligosaccharides encompassed linear sequences with homo (single) linkages: 1,2-, 1,3-, 1,4- ,or 1,6- with α or β configurations; and hetero (multiple) linkages: 1,3-, 1,4, or 1,6-; also branched oligosaccharide sequences with 1,3 and 1,6-linkages.

To our knowledge, this is the first sequence-defined glycome-scale microarray constructed. We used 12 selected proteins (antibodies and CBMs) known to target α- or β-glucans to validate the approach. We then applied the microarray analysis to Dectin-1 and DC-SIGN, which revealed new insights into the specificities of these signaling molecules of the innate immune system.

EXPERIMENTAL PROCEDURES

Materials—The proteins investigated and their reported oligosaccharide recognition with references are given in supplemental Table
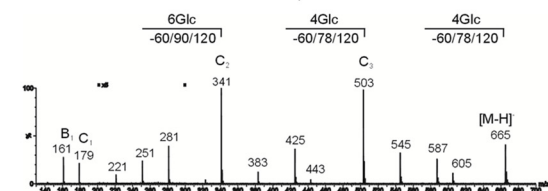
---

[1] The abbreviations used are: CBM, carbohydrate-binding module; NGL, neoglycolipid; DP, degree of polymerization; DC-SIGN, dendritic cell-specific ICAM-3-grabbing nonintegrin; CAZy, Carbohydrate-Active enzyme.
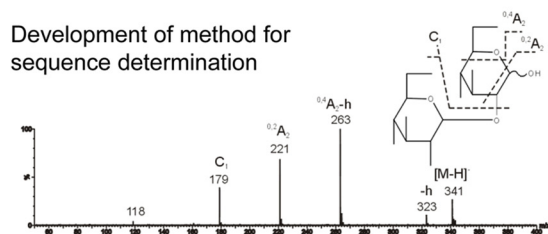
FIG. 1. **Neoglycolipid (NGL)-based designer glucome microarray with mass spectrometry as a tool to assign carbohydrate ligands in glucan recognition.** Ligand-bearing glucan polysaccharides, described in supplemental Fig. S1 and Table S1, were selected as sources of gluco-oligosaccharides for construction of the microarray. A total of 121 gluco-oligosaccharide fractions were obtained with different DP after partial depolymerization of polysaccharides and fractionation. ESI-CID-MS/MS method was developed using gluco-oligosaccharides with known sequences and applied to determination of sequences of oligosaccharide fragments from polysaccharides. Gluco-oligosaccharides were converted to NGL probes for microarray construction and interrogation with the glucan-recognizing proteins described in supplemental Table S2.

S2. The details of proteins investigated and the polysaccharide and oligosaccharide sources for preparation of glucan oligosaccharide fractions, together with the other chemically synthesized and commercially available gluco-oligosaccharides, are described in supplemental Methods.

Preparation of Oligosaccharide Fractions from Gluco-Fructosides and Glucan Polysaccharides—Gluco-oligosaccharide mixtures with differing chain lengths prepared by partial depolymerization of gluco-oligosaccharide fructosides or polysaccharides using acid or enzyme

hydrolysis (as described below and summarized in supplemental Table S1) were fractionated by gel filtration chromatography on a Bio-Gel P4 or P6 column (1.6 × 90 cm) eluted with deionized water at a flow rate of 15 ml/h. Alternatively, when the hydrolysates were in limited amounts, a Superdex-Peptide FPLC column (Pharmacia Biotech, Uppsala) was used for fractionation at a flow rate of 0.3 ml/min. The eluates were monitored on-line by refractive index, and pooled according to their glucose units, as determined by MALDI-MS. Quantitation of oligosaccharide fractions was by dot-orcinol assay (24)

using glucose as standard. Unless otherwise specified, oligosaccharide fractions that contained flanking shorter or longer components additional to the major components were not resolved further. The sizes and compositions of the oligosaccharide fractions are indicated in supplemental Table S6*A*/*B*, which give the results of MALDI-MS analyses of the NGL probes derived from each of the oligosaccharide fractions.

Cyanobacterium gluco-oligosaccharide fructosides were subjected to mild acid hydrolysis with 0.5 M TFA at 95 °C for 9 min to remove the fructose as described (38). Partial depolymerization of the gluco-oligosaccharides was then carried out with 0.5 M TFA at 95 °C for 140 min. TFA was removed by repeated coevaporation with MeOH; this was followed by fractionation by FPLC to obtain α1,2-linked gluco-oligosaccharides with Glc_2 to Glc_9 as major components (Cyano-2 to Cyano-9, respectively).

Poria cocos glucan (Poria) was hydrolyzed with 10 mM TFA at 100 °C for 2 h. TFA was removed by repeated coevaporation with MeOH, and oligosaccharides were fractionated by FPLC. The high oligomers (>DP-20) recovered from chromatography were retreated with 10 mM TFA as above and rechromatographed, and the procedures were repeated twice. The hydrolysates were then combined and subjected to Bio-Gel P4 chromatography to obtain 12 α1,3-linked gluco-oligosaccharide fractions, Poria-2 to Poria-13. Contaminating α1,4-linked gluco-oligosaccharides (supplemental Results) were removed by preparative high-performance (HP) TLC, having observed that the 1,4-linked malto-oligosaccharides migrate slower than the α1,3-linked oligosaccharides (supplemental Fig. S6*B*), using aluminum-backed silica gel HPTLC plates (Merck) and a solvent system *n*-propanol/H_2O 7:3 (by volume). The plates were developed twice, and the slower-migrating α1,4-linked contaminants were removed. The purified oligosaccharides were analyzed by HPTLC and MALDI-MS, and results with the Poria-7 fraction before and after HPTLC purification are shown in supplemental Fig. S6*B* and 6*C*. A series of α1,3-linked oligosaccharide fractions 3 to 13, was thus obtained, with Glc_3 to Glc_{13} as major components (Poria-3 to Poria-13) (supplemental Results and Tables S7*A*).

A pool of malto-oligosaccharides obtained by acid hydrolysis of maltodextrins was from V-LABS (Covington, LA) and used directly for Bio-Gel P4 fractionation to obtain a series of α1,4-linked oligosaccharide fractions 8 to 13, with Glc_8 to Glc_{13} as the major components (Malto-8 to Malto-13).

Dextran oligosaccharide mixture was obtained by treatment of the polysaccharide (20 mg/ml) with 0.1 M HCl at 100 °C for 4 h. The reaction was stopped by cooling to room temperature and neutralization with equimolar NaOH solution. Desalting was performed by a short mixed-bed cation (AG50 $\times$ 8) and anion (AG1 $\times$ 8) exchange column. The desalted reaction mixture was subjected to Bio-Gel P4 fractionation to obtain α1,6-linked oligosaccharide fractions 2 to 13 with Glc_2 to Glc_{13} as the major components (Dext-2 to Dext-13).

Linear β1,2 oligosaccharides derived from CβG were obtained by hydrolysis with 0.01 M HCl at 100 °C for 2 h after the removal of succinyl side chains by treatment with 0.1 M NaOH (details will be described by HZ and colleagues elsewhere). The reaction was stopped by cooling to room temperature and neutralization with equimolar aqueous NaOH solution. Desalting was performed by gel filtration with a short (1.6 $\times$ 30 cm) Sephadex G10 column and the oligosaccharides were fractionated by Bio-Gel P4 to obtain β1,2-linked fractions 2 to 13 with Glc_2 to Glc_{13} as the major components (CβG-2 to CβG-13).

An acid hydrolysate of curdlan was obtained from Megazyme (Wicklow, Ireland) to isolate the minor longer oligomers. The hydrolysate was enriched for DP-8 to DP-13 by ultrafiltration (molecular weight cut-off 1000) before Bio-Gel P4 chromatography to obtain β1,3-linked fractions, 8 to 13, with Glc_8 to Glc_{13} as the major components (Curd-8 to Curd-13).

The acid hydrolysate of cellulose was prepared by controlled acid hydrolysis of cellulose acetate and was provided by Megazyme. The oligosaccharide mixture was fractionated by Bio-Gel P4 to obtain β1,4-linked fractions 2 to 13 with Glc_2 to Glc_{13} as the major components (Cello-2 to Cello-13).

Pustulan (at 10 mg/ml) was treated with 0.2 M HCl at 100 °C for 8 h. The reaction was stopped by cooling to room temperature and neutralization with equimolar aqueous NaOH solution. Desalting was performed by gel filtration with a short Sephadex G10 column, before oligosaccharide fractionation by Bio-Gel P6 to obtain β1,6-linked fractions. HPTLC analysis of the fractions showed that size heterogeneity was high and semipreparative HPTLC was used to enrich for DP-2 to DP-8 (Pust-2 to Pust-8) (results not shown). Purification of oligosaccharide fractions 9–13 proved not possible, and these were used without further fractionation. There was evidence of α-linked mannose contaminant as detected by binding signals with ConA in microarray analysis (supplemental Table S7*B*) of these fractions. The mannose contaminant is considered minor (2% or less) as mannose was not detected on the polysaccharide or on fraction 10 by NMR. Therefore, fractions 9 to 13 are considered to contain Glc_9 to Glc_{15} as the major components (Pust-9 to Pust-15), as shown in supplemental Table S6*A*.

Barley oligosaccharide mixture was obtained by hydrolysis of barley β-glucan with a novel cellulase with high transglycosylation activity (Novozyme) at 37 °C for 30 min. The digest was fractionated by Bio-Gel P4 to obtain oligosaccharide fractions 3 to 16 with Glc_3 to Glc_{16} as major components (Barley-3 to Barley-16) with mixed β1,3 and β1,4-linkages.

Hydrolysis of grifolan and lentinan was carried out with 0.02 M TFA at 100 °C for 12 h. After cooling to room temperature, the hydrolysate mixture was centrifuged. The supernatant was coevaporated with MeOH and fractionated by a short (1.6 $\times$ 36 cm) column of Bio-Gel P6. The high (>DP-20) and low (< DP-20) oligomer fractions, as determined by MALDI-MS, were kept separately. The precipitate and high oligomer fractions were combined and the TFA treatment procedure was repeated three times to increase the yield of low oligomers. The low oligomer fractions were combined and subjected to a final gel filtration to obtain, from grifolan, fractions 2 to 16 with Glc_3 to Glc_{16} as major components (Grifo-3 to Grifo-16) and from lentinan fractions 2 to 13, with Glc_2 to Glc_{13} as major components (Lenti-2 to Lenti-13). Microarray binding data with the α1,4-glucose specific *Tm*CBM41 (Fig. 5*B* and supplemental Table S7*B*) indicated the presence of a minor α1,4-linked glucose contaminant in the lentinan fractions, particularly those containing oligomers with >DP-8 as major components. This was corroborated by MS/MS (footnote in supplemental Table S7*A*) and NMR (not shown).

Electrospray Mass Spectrometry—For glucose linkage and oligosaccharide sequence analyses, negative-ion ESI-MS and ESI-CID-MS/MS were carried out on a Micromass Q-TOF mass spectrometer (Manchester, UK). Nitrogen was used as desolvation and nebulizer gas at a flow rate of 250 l/h and 150 l/h, respectively. Source temperature was 80 °C, and the desolvation temperature 150 °C. A cone voltage of 50 V was used for negative-ion detection and the capillary voltage was maintained at 3 kV. MS/MS product-ion spectra were obtained from CID using argon as the collision gas at a pressure of 0.17 MPa. The collision energy was adjusted between 17 and 28 V for optimal fragmentation. For quasi-MS^3 to obtain a further product-ion spectrum from a selected fragment ion as the precursor, the cone voltage was raised to 80 V to encourage the primary fragmentation. A scan rate of 1.0 s/scan and data acquisition of ~1 min were used for both ES-MS and ES-CID-MS/MS experiments, and the acquired spectra were summed for presentation. For analysis, oligosaccha-

rides were dissolved in ACN/water (1:1, v/v), typically at a concentration of 15 pmol/μl, of which 2 μl was loop injected. Solvent (ACN/2 mM NH$_4$HCO$_3$, 1:1, v/v) was delivered by a Harvard syringe pump at a flow rate of 10 μl/min.

MALDI Mass Spectrometry—MALDI-MS was carried out for molecular mass determination of gluco-oligosaccharides and NGLs on a Tof Spec-2E instrument (Waters, Manchester, UK). The oligosaccharides were dissolved in H$_2$O and NGLs in CHCl$_3$/MeOH/H$_2$O (25:25:8), at a concentration of ~10 pmol/μl, and 0.5 μl was deposited on the sample target together with a matrix of 2′,4′,6′,-trihydroxyacetophenone for analysis. Laser energy was 100% (coarse) and 50% (fine); resolution was at 1000.

NMR Analyses—For determination of sequence and anomeric configuration by NMR, glucan polysaccharides and oligosaccharides investigated (500 μg of each) were taken up in D$_2$O 99.9% (Apollo Scientific, Stockport, UK) exchanged by lyophilisation, then redissolved in 0.3 ml D$_2$O and transferred to a 5 mm small-volume NMR tube (Shigemi, Tokyo, Japan). NMR spectra were recorded at 600 MHz, 30 °C on either a Varian I nova or a Bruker Avance spectrometer, or at 700 MHz using a Bruker Avance spectrometer equipped with cryoprobe. 1D and 2D pulse sequences were supplied by the equipment manufacturer. Chemical shifts are given relative to acetone at 2.213 ppm (^{1}H) and 33.0 ppm (^{13}C).

Saturation Transfer Difference (STD) NMR—Oligosaccharide samples were prepared to a concentration of 1 mM in 10 mM phosphate buffer, pH 7.2, and exchanged by lyophilisation before transfer to a 5 mm NMR tube. Protein was added to a concentration of ~5 μM, yielding a protein/oligosaccharide ratio of about 1:100. Spectra were recorded at 700 MHz using a Bruker Avance spectrometer equipped with a cryoprobe, at a temperature of either 30 °C or 45 °C. Selective saturation was achieved using a 50 ms adiabatic inversion pulse train irradiating a 950 Hz (1.36 ppm) window at 50 ppm for off-resonance irradiation and typically 7.5 ppm, and -0.3 ppm for protein irradiation. 32 transients of 16K complex points were collected for each irradiation frequency. Processing and subtraction were performed in either Bruker Topspin software or in MNova (Mestrelab Research, Santiago di Compostela, Spain). STD enhancements were calculated as a percentage of the unperturbed spectrum for each individual experiment; where the results of more than one experiment were combined, normalized values were used to improve precision.

Gluco-Oligosaccharide NGLs—Gluco-oligosaccharides were converted to NGLs by oxime-ligation using the lipid reagent *aminooxy*-functionalized 1,2-dihexadecyl-*sn*-glycero-3-*p*hosphoethanolamine (AOPE) essentially as described (39). In brief, for gluco-oligosaccharides of ≤DP-7 oligosaccharides (100 nmol) were dried and incubated with AOPE (200 nmol) in a solvent (~50 μl) of CHCl$_3$/MeOH/H$_2$O (10:10:1, by vol) at ambient temperature for 16 h before solvent evaporation slowly (over the course of 1 h) at 60 °C; for the larger oligosaccharides (>DP- 7) of Malto-, Dext-, Curd-, and Cello- series, and Pust-oligosaccharide DP-8, ten equivalents of AOPE were applied and incubation was prolonged to 24 h under acidic conditions (CHCl$_3$/MeOH/water/acetic acid, 25:25:8:1) at 60 °C. A modified procedure (details will be described by HZ and colleagues elsewhere) was used for the large oligosaccharides that are particularly hard to dissolve (Pust-series >DP-8; Cyano-, Poria-, CβG-, Barley-, Grifo-, and Lenti-series >DP-7 and the synthetic linear and branched gluco-oligosaccharides). NGLs of β1,4-linked mannose and xylose oligosaccharides, used as controls, were from the Glycosciences library of probes prepared by reductive amination with the amino lipid, 1,2-dihexadecyl-sn-glycero-3-phosphoethanolamine (DHPE) (40). Purification of the NGLs from reaction mixtures(40) was carried out by semipreparative HPTLC for gluco-oligosaccharides in the range of DP-2 to DP-6, and silica gel cartridge for >DP-7. The purified NGLs were analyzed by MALDI-MS (supplemental Table S6A-6C)

and HPTLC before quantitation by primulin staining on HPTLC plates (40).

Carbohydrate Microarray Analyses—The information on the probe ID, sequence and glucose-DP for the 158 NGLs included in the microarrays is shown in supplemental Table S7A. The NGLs were printed onto 16 pad nitrocellulose-coated glass slides using a non-contact robotic arrayer in duplicate at two levels, 2 and 5 fmol/spot, following established protocols (41). The binding signals elicited with the proteins were related to dose of probe arrayed; the results at 5 fmol/spot are presented throughout. Microarrays of polysaccharides were also constructed for analyses of the binding with the proteins investigated (supplemental Fig. S1). The polysaccharides were taken up in water, with the exception of curdlan polysaccharide that was solubilized using mild alkaline solution (50 mM NaOH), and printed onto 16 pad nitrocellulose-coated glass slides at a final concentration of 0.1 and 0.5 mg/ml.

Microarray binding analyses were performed using AlexaFluor-647-labeled Streptavidin for readout, essentially as described (41). The His-tagged proteins were analyzed precomplexed with mouse monoclonal anti-poly-histidine (Ab1) and biotinylated anti-mouse IgG antibodies (Ab2), both from Sigma, at a ratio of 1:3:3 (by weight). The protein–antibody complexes were prepared by preincubating Ab1 with Ab2 for 15 min at ambient temperature, followed by addition of proteins and incubation for a further 15 min and diluted to the final concentration of the proteins in the blocking solution made of 3% (w/v) BSA from Sigma (A8577) in HBS (5 mM HEPES buffer pH7.4, 150 mM NaCl) with 5 mM CaCl$_2$ (Blocker A). The final concentrations of the proteins were: 15 μg/ml for murine and human Dectin-1; 2 μg/ml for *Bh*CBM-6 and *Tm*CBM4–2; 1 μg/ml for *Cm*CBM6–2 and *Tm*CBM41; 5 μg/ml for *Cm*CBM32–2 and *Ct*CBM11.

The Fc-tagged murine Dectin-1 and DC-SIGN were analyzed without precomplexing (at 20 and 2 μg/ml, respectively) in the blocking solution Casein (Pierce) diluted to 0.5% in HBS (Blocker B, for Fc-Dectin-1) and in the blocking solution Casein diluted to 0.02% in HBS with addition of 1% BSA and 5 mM CaCl$_2$ (Blocker C, for Fc-DC-SIGN), followed by the biotinylated goat anti-human-IgG (Vector) at 10 μg/ml in the respective blocking solution for each protein.

The antibodies were analyzed without precomplexing: 2G8-IgG and 1H8-IgG at 0.1 μg/ml and 1E12-IgM at 0.2 μg/ml in Blocker C, followed by the biotinylated anti-mouse-IgG or anti-mouse-IgM as appropriate, both from Sigma at 10 μg/ml in the same blocker; MOPC 104-E-IgM at 3 μg/ml in Blocker A, followed by the biotinylated anti-mouse-IgM (Sigma) at 10 μg/ml in the same blocker. The biotinylated proteins were analyzed using a single step overlay; these included anti-dextran m3.41G6 and m16.4.12E at 1:500 in Blocker C; and ConA at 2 μg/ml in Blocker A.

Microarray data analysis was performed using a dedicated software (42) developed by Mark Stoll of the Glycosciences Laboratory.

RESULTS

Development of Negative-Ion ESI-CID-MS/MS Method for Linkage and Sequence Determination of Gluco-Oligosaccharides

Diagnostic Fragmentation for Different Glycosidic Linkages— For method development to determine at high-sensitivity (low pmol) the linkages and sequences in gluco-oligosaccharides, eight disaccharides were used that represent naturally occurring glucose linkages, including 1,2-, 1,3-, 1,4-, and 1,6- with both α- and β-configurations (Table IA).

The product-ion spectra of the four α-anomeric disaccharides with 1,2-, 1,3-, 1,4-, and 1,6-linkages are shown in Fig.

TABLE I

Fragmentations of gluco-disaccharides observed in negative-ion ESI-CID-MS/MS product-ion spectra to establish the features of fragmentation of gluco-oligosaccharides

(*A*) Major fragment ions observed.

Disaccharides	Sequence	Cross-ring cleavage					Glycosidic cleavage
		−18	−60	−78	−90	−120	−162
Kojibiose	Glcα1,2Glc	[M−H]−h	–	$^{0,4}A_2$−h	–	$^{0,2}A_2$	C_1
Sophorose	Glcβ1,2Glc	[M−H]−h	–	$^{0,4}A_2$−h	–	$^{0,2}A_2$	C_1
Nigerose	Glcα1,3Glc	–	–	–	–	–	C_1
Laminaribiose	Glcβ1,3Glc	–	–	–	–	–	C_1
Maltobiose	Glcα1,4Glc	–	$^{0,2}A_2$	$^{0,4}A_2$−h	–	$^{2,4}A_2$	C_1
Cellobiose	Glcβ1,4Glc	–	$^{0,2}A_2$	$^{0,4}A_2$−h	–	$^{2,4}A_2$	C_1
Isomaltobiose	Glcα1,6Glc	[M−H]−h	$^{0,2}A_2$	–	$^{0,3}A_2$	$^{2,4}A_2$	C_1
Gentiobiose	Glcβ1,6Glc	[M−H]−h	$^{0,2}A_2$	–	$^{0,3}A_2$	$^{2,4}A_2$	C_1

(*B*) Diagnostic neutral losses of A-type fragmentation giving the distinctive fragment ion set for different linkages of gluco-disaccharides, also applicable to oligosaccharides.

A-type neutral losses*	Linkage
−18/78/120	-2Glc
–	-3Glc
−60/78/120	-4Glc
−60/90/120	-6Glc

* The fragmentation ions are counted from the molecular ion [M-H]$^-$ and glycosidic C-ions; '-' indicates not detected.

2*A*-2*D*. Under the conditions selected each glucose linkage isomer had a different fragmentation pattern. Glycosidic C-type (43) cleavages resulting in fragment ions C_1 at m/z 179, arising from a neutral loss of 162 Da from the molecular ion at m/z 341, were observed in the spectra of all disaccharides but with different relative intensities. A-type fragmentation across the saccharide ring gave particularly useful information on the linkages: In the spectrum of the α1,2-linked kojibiose (Fig. 2*A*), neutral losses of 18, 78 and 120 Da gave a distinctive set of three ions at m/z 323, 263 and 221, as [M−H]$^-$-h, $^{0,4}A_2$-h, and $^{0,2}A_2$, respectively (-h denotes dehydration). For the α1,3-linked nigerose, glycosidic cleavage C_1 only was observed at m/z 179, whereas A-type fragmentation was absent (Fig. 2*B*). The α1,4- and α1,6-linked disaccharides each produced extensive A-type fragmentation in addition to the C_1 ions: in the spectrum of the α1,4-linked maltobiose (Fig. 2*C*) these were the $^{0,2}A_2$ (m/z 281), $^{0,2}A_2$-h (m/z 263), and $^{2,4}A_2$ (m/z 221) arising from neutral losses of 60, 78 and 120 Da, respectively, whereas in the spectrum of α1,6-linked isomaltobiose (Fig. 2*D*), these were the $^{0,2}A_2$ (m/z 281), $^{0,3}A_2$ (m/z 251), and $^{0,4}A_2$ (m/z 221) arising from neutral losses of 60, 90, and 120 Da, respectively. The β-anomers of the 1,2-, 1,3-, 1,4-, and 1,6-linked disaccharides (Table I*A*) gave product-ion spectra (not shown) almost identical to those of their α-anomers.

In sum, under the conditions established, each linkage produced a unique set of fragments that can be used for assignment of the glucose linkages: A-type fragmentation with neutral losses of 18/78/120 Da for 1,2-linkage, 60/78/120 Da for 1,4-linkage, and 60/90/120 Da for 1,6-linkage; the absence of A-fragment is indicative of a 1,3-linkage (Table I*B*).

Linear Sequences with Homo-Linkages—We next investigated if the distinctive fragmentation patterns derived from disaccharides with single linkage can be extended to longer chains. Each of the linear heptasaccharides with different linkages that were used as representatives (supplemental Table S3) were found to give uniquely different spectra, with a fragmentation pattern similar to the corresponding disaccharide (Fig. 2*E*-2*H* and supplemental Results). In the cases where fragment ions were weak or absent in the lower mass regions and insufficient to make unambiguous linkage assignment, as for the α1,4-linked Malto-7 (Fig. 2*G*) and α1,6-linked Dext-7 (Fig. 2*H*), further product-ion scanning using C-ions as the precursors (quasi MS^3) revealed the complete linkage information: C_4 ions (m/z 665) were fragmented (supplemental Fig. S2), producing similar but stronger A-type fragment ions in the lower mass region, indicating 1,4 and 1,6-linkages, respectively.

Linear Sequences with Hetero-Linkages—The principles established above were used to assess the utility of the method for sequencing linear gluco-oligosaccharides containing different linkage types. Pullu-4 has two 1,4-linkages and one 1,6-linkage (supplemental Table S3). The product-ion spectrum (Fig. 3*A*) can be used to assign the three individual linkages as well as their locations. The two A-ion sets derived from losses of 60/78/120 recorded from the two consecutive residues at the reducing side were identical to the fragmentation pattern for the 4-linked Glc (Table I*B*), corresponding to two 1,4-linkages. The ion set with -60/90/120 from C_2 (m/z 341) (Table I*B*) can be used to assign the nonreducing terminal 1,6-linkage. Other α1,4/α1,6-linked gluco-oligosaccharides Pullu-7 (supplemental Fig. S3) and the isomeric trisaccharide pair Pano-3 and i-Pano-3 (supplemental Fig. S4) can also be readily identified.

Barley oligosaccharides contain β1,3/β1,4-linkages (supplemental Table S3). The A-ion set -60/78/120 was similarly used to assign the 4-linkage and the lone glycosidic C-ion was used to identify the 3-linkage as shown in the spectrum of Barley-4c (Fig. 3*B*) and -4b (Fig. 3*C*).
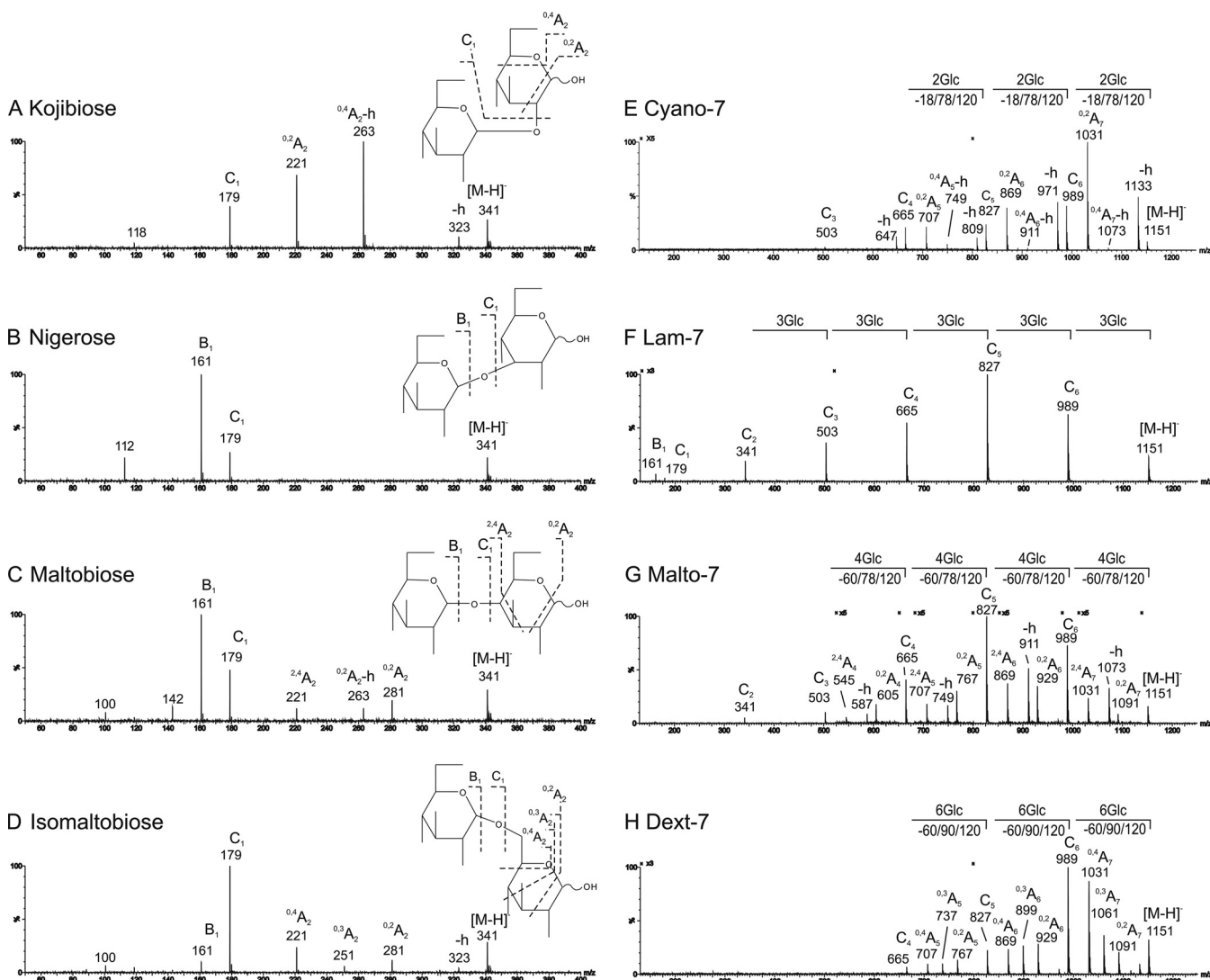
FIG. 2. **Negative-ion ESI-CID-MS/MS product-ion spectra of gluco-disaccharides and linear gluco-heptasaccharides with homo-linkages.** (*A*) Kojibiose with an α1,2-linkage. (*B*) Nigerose with an α1,3-linkage. (*C*) Maltobiose (Malto-2) with an α1,4-linkage. (*D*) Isomaltobiose with an α1,6-linkage. (*E*) Cyano-7 with α1,2-linkages. (*F*) Lam-7 with β1,3-linkages. (*G*) Malto-7 with α1,4-linkages. (*H*) Dext-7 with α1,6- linkages.

Branched Sequences—We further investigated the capacity of our approach to branching pattern analysis. Four branched oligosaccharides with a single or double Glcβ1,6-branch on β1,3-nonasaccharide backbone (supplemental Table S3) were also used to assess the approach. The product-ion spectra (Fig. 3*D*-3*F* and supplemental Fig. S5) showed distinctive fragmentation patterns: Only C-type cleavage occurred indicating 3-linkage along the backbone and the gap of 324 Da, equivalent to two Glc units (162 × 2) within the full sets of C-ions could be used for location of the branching point.

Collectively, the product-ion spectra of the oligosaccharides analyzed demonstrated the utility of the negative-ion ESI-CID-MS/MS method for sequence determination of single or mixed linkages in linear and branched gluco-oligosaccharides, as well as their locations within the oligosaccharide chain.

Application of ESI-CID-MS/MS to Sequence Determination and Mixture Analysis

The method established was used for sequence determination of representative oligosaccharide preparations in each linkage series (as indicated in supplemental Table S7A). Unsuspected gluco-oligosaccharide sequences were also revealed. Two examples are given below as representatives.

The pentasaccharide Barley-5a was isolated from barley β-glucan after digestion with a novel cellulase. The sequence was predicted to be Glcβ1,3Glcβ1,4Glcβ1,4Glcβ1,4Glc. However, in addition to 1,4-linkage with ion set -60/78/120 and nonreducing 1,3-linkage with absence of A-fragments, there was an A-type ion set -60/90/120 in spectrum, identifying an internal 1,6-linkage (Fig. 4*A*). The sequence could be assigned as Glcβ1,3Glcβ1,4Glcβ1,6Glcβ1,4Glc, which was
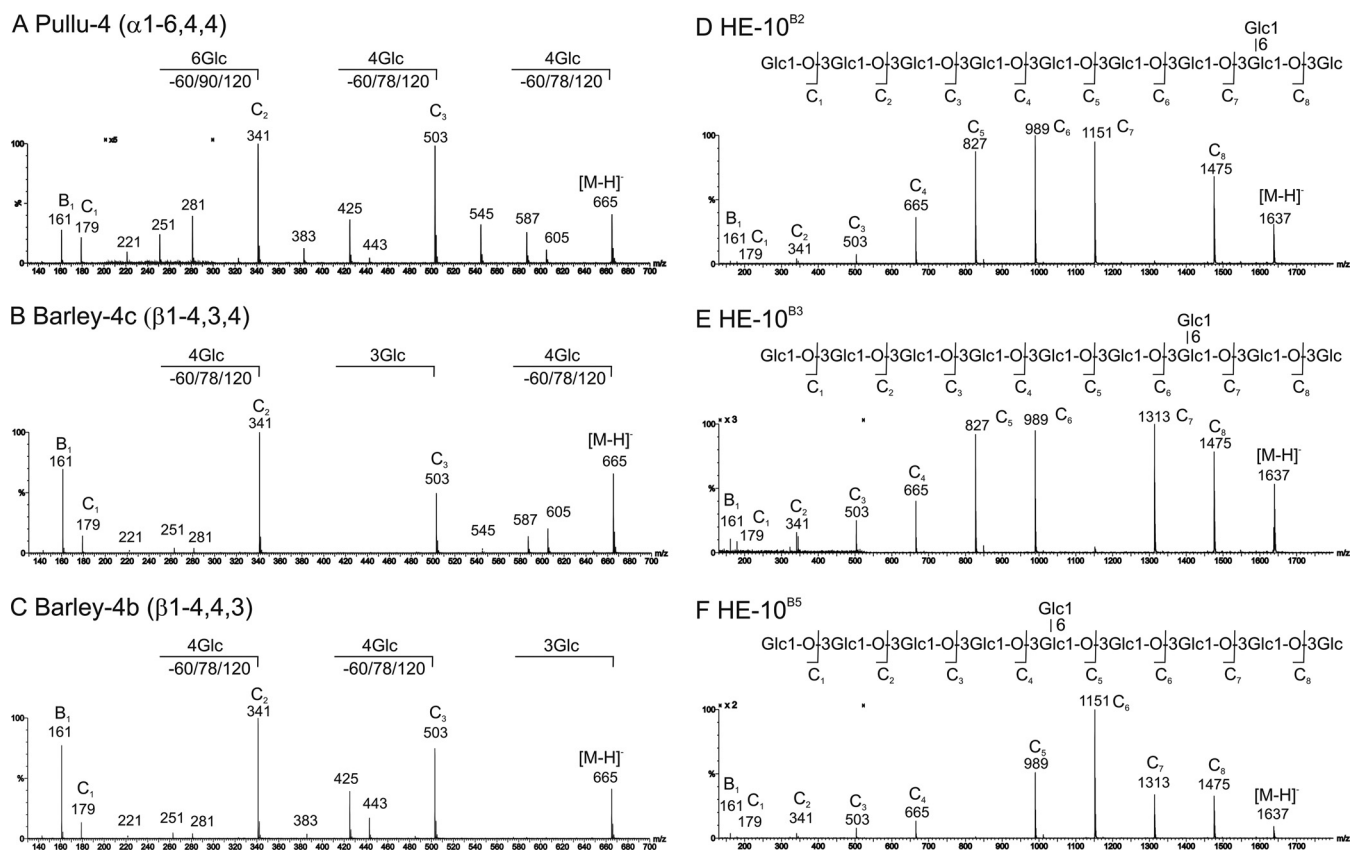
FIG. 3. **Negative-ion ESI-CID-MS/MS product-ion spectra of linear gluco-tetrasaccharides with mixed linkages and branched gluco-decasaccharides.** (*A*) Pullu-4 (α1,6,1,4,4 linkages). (*B*) Barley-4c (β1,4,1,3,1,4 linkages). (*C*) Barley-4-b (β1,4, 1,4, 1,3 linkages). (*D*) HE-10^{B2}. (*E*) HE-10^{B3}. (*F*) HE-10^{B5}.

corroborated by NMR (supplemental Results and supplemental Table S4).

The *Poria cocos* polysaccharide (44) was selected as a source of α1,3-linear gluco-oligosaccharides. However, the product-ion spectrum of the isolated Poria-7 fraction showed not only C-ions consistent with 1,3-linkage but also weak A-type ions at -60/78/120 typical of 1,4-linkage (Fig. 4*B* and supplemental Results). These results, together with initial microarray binding data with the α1,4-glucose specific *Tm*CBM41 (supplemental Table S2), showing unpredicted binding to Poria-oligosaccharide fractions analyzed as NGLs (supplemental Fig. S6*A*), indicated the presence of a α1,4-linked glucose contaminant. This was corroborated by NMR (supplemental Table S5). After repurification, there were no longer signals for 1,4-linked glucose in the spectrum, and *Tm*CBM41 binding signals were greatly reduced, indicating that the contaminant was largely removed.

Construction and Validation of the Glucome Microarray as a Tool for Analysis of Glucan-Recognition

Representative gluco-oligosaccharide fractions (*e.g.* the heptasaccharide fractions) prepared in each series were sequenced by the ESI-CID-MS/MS and the results corroborated by NMR (data not shown). The oligosaccharides were then converted into NGL probes by oxime-ligation to an aminooxy-functionalized-lipid. The oxime-linked NGLs have a significant proportion of the lipid-linked monosaccharide cores in ring-closed form as there is no reduction involved in the conjugation reaction (39). The conditions for preparation of the NGLs from the large oligosaccharides ($>$DP-7) were optimized in order to overcome the well-known solubility problem, particularly with the long chain gluco-oligosaccharides. The NGLs were analyzed by MALDI-MS (supplemental Tables 6*A*-6*C*). The 153 gluco-oligosaccharide NGLs together with five xylo- and manno-oligosaccharide NGLs as controls (supplemental Table S7*A*) were printed on nitrocellulose-coated glass slides at 2 and 5 fmol/spot.

For validation, the microarray was probed with 12 glucan-recognizing proteins: six monoclonal antibodies (mAbs) and six microbial CBMs for which the recognition features had been described using different methods; these, together with the respective references, are summarized in supplemental Table S2. The reported features were used for validation. Additional specificities were also revealed using the newly constructed microarrays. Salient findings are described below.

Narrow Binding Profiles of Anti-α-glucan Antibodies—Three mAbs had highly restricted binding to linear α-linked se-
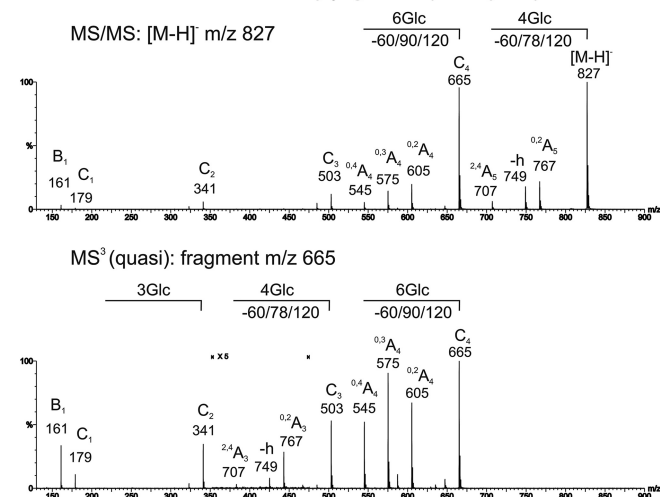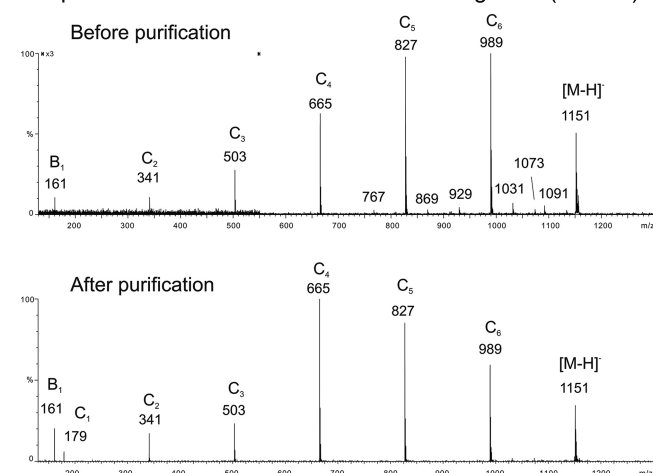
A Pentasaccharide from barley β-glucan (Barley-5a)

B Heptasaccharide fraction from *Poria cocos* glucan (Poria-7)

FIG. 4. **Application of the negative-ion ESI-CID-MS/MS method to sequence determination and in detection of unsuspected gluco-oligosaccharide sequences.** (*A*) MS/MS (upper panel) and quasi-MS³ (lower panel) for sequencing a pentasaccharide Barley-5a isolated from barley β-glucan hydrolysate. (*B*) MS/MS of Bio-Gel P4 fraction of *Poria cocos* glucan oligosaccharide, Poria-7, before (upper panel) and after (lower panel) removal of minor contaminant by semi-preparative HPTLC.

quences (Fig. 5*A* and supplemental Tables S7*A*/*B*). MOPC myeloma 104-E-IgM showed binding exclusively to linear α1,3-oligosaccharides, particularly strongly to DP-4 to DP-8. The anti-α1,6-dextran hybridoma antibodies, 16.412E-IgA (cavity-type) and 3.4.1G6-IgG3 (groove-type), showed the predicted binding to α1,6-dextran oligosaccharides, >DP-3 and >DP-5, respectively. The 16.4.12.E-IgA differed and showed additional binding to Pullu-4 and -7 (probes 52 and 53, supplemental Tables S7*A*/*B*), which have in common the tetra-saccharide sequence Glcα1,6Glc1,4Glc1,4Glc with α1,6-linkage at their nonreducing termini. This indicates that the cavity-type antibody 16.4.12.E-IgA recognizes the nonreducing terminal capping α1,6-disaccharide motif and that the internal

α1,4-linked trisaccharide can serve to present this motif without interfering. However, the groove-type 3.4.1G6-IgG3 requires 1–6 linkage throughout the chains. The weak binding signals observed with the probe derived from the β1,2-linked DP-11 with both antibodies are unexplained and require investigation.

Binding Profiles of Vaccine-Induced Anti-β-glucan Anti-bodies—The murine hybridoma antibodies 2G8-IgG, 1H8-IgG and 1E12-IgM, induced upon immunization with a *Candida albicans* β-glucan, bound exclusively to β-linked sequences (Fig. 5*A*). Antibodies 2G8-IgG and 1H8-IgG bound only to β1,3-gluco-oligosaccharides (>DP-3 or DP-4) among the linear sequences, whereas the 1E12-IgM gave binding to all β-linked sequences as short as DP-2, weakest of all to β1,2-linked. Both IgG antibodies also bound to the β1,3/β1,6-branched gluco-oligosaccharides derived by chemical synthesis or isolated from branched polysaccharides. However, the binding was relatively weak compared with linear sequences of the same chain length (see also supplemental Fig. S9). The IgM antibody, unlike the IgG antibodies, gave robust binding to the synthetic di-branched tetrasaccharide probe 157 (supplemental Tables S7*A*/*B*). The internal α-linkage of this probe is clearly not accommodated by the two IgG antibodies, indicating their requirement for contiguous (>DP-3/-4) β1,3-linked sequences.

Footprints of Glucan Binding by Microbial CBMs—The six glucan-binding CBMs analyzed belong to different CAZy families (supplemental Table S2 and references therein).

*Tm*CBM41 showed the predicted binding to α1,4-gluco-oligosaccharides (Fig. 5*B*). Strong binding was detected with four pullulan-derived linear α1,4/α1,6-linked oligosaccharides (probes 50–53, supplemental Tables S7*A*/*B*). The binding signal intensities with i-Pano-3 (Glcα1,4Glcα1,6Glc) and Pullu-7 (Glcα1,6Glcα1,4Glcα1,4Glcα1,6Glcα1,4Glcα1,4Glc) were comparable to those of α1,4-linked gluco-oligosaccharides of the same size. However, binding was not detected to isomeric Pano-3 (Glcα1,6Glcα1,4Glc) or Pullu-4 (Glcα1,6Glcα1,4Glcα1,4Glc). This provides new evidence that internal α1,6-linkage is better tolerated than that at the non-reducing end by this CBM.
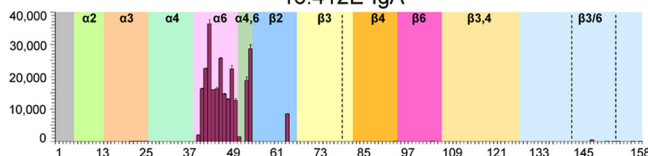
*Ct*CBM11 showed binding exclusively to barley-derived oligosaccharides (Fig. 5*B*), in agreement with the reported high affinity to barley-derived tetrasaccharide Glcβ1,4Glcβ1,4Glcβ1,3Glc with a reducing terminal 3-linkage. However, in the microarray analysis only DP-7 (Glcβ1,4Glcβ1,4Glcβ1,3Glcβ1,4Glcβ1,4Glcβ1,3Glc) and longer chain probes were bound (probes 116–125, supplemental Tables S7*A*/*B*). The reported weak affinity to linear β1,4-linked oligosaccharides was not detected here, which may indicate that both the sequence of β1,4-linkages adjacent to a β1,3-linked glucose and chain length are important for recognition. This could also explain the lack of binding to Glcβ1,4Glcβ1,4Glcβ1,3Glc (probe 108) as mentioned above, as the conjugation of reducing end glucose of this tetrasaccharide to the lipid may have hindered access of the protein to the binding epitope.
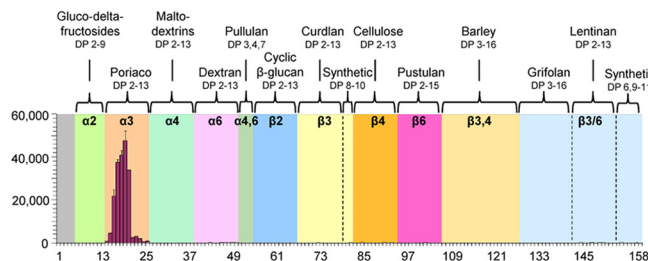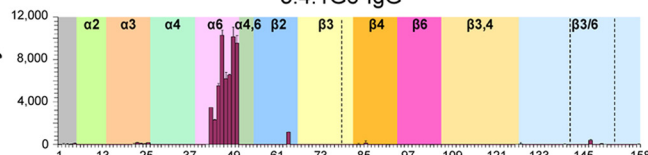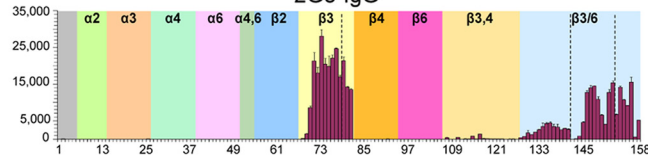
FIG. 5. **Validation of the glucome microarray with 12 glucan-recognizing proteins.** (*A*) Murine monoclonal antibodies that recogn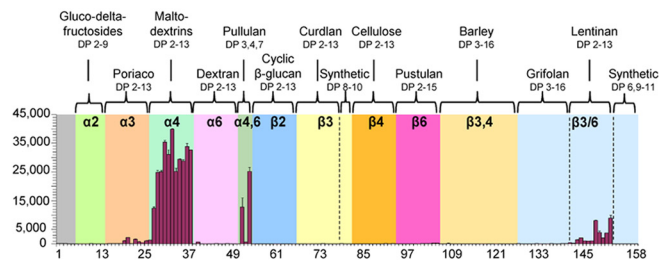ize α- or β-glucans: MOPC-104E-IgM, 16.4.12.E-IgA, 3.4.1G6-IgG3, 2G8-IgG, 1H8-IgG and 1E12-IgM. (*B*) CBMs of microbial glycoside hydrolases of different CAZy families: *Tm*CBM41, *Ct*CBM11, *Tm*CBM4–2, *Cm*CBM32–2, *Bh*CBM6 and *Cm*CBM6–2. The microarrays included 153 gluco-oligosaccharide-NGLs for which the glucose linkages are indicated in the colored panels; these were linear sequences with homo linkages: 1,2-, 1,3-, 1,4-, or 1,6-linked, with α or β configurations in the size range mostly of DP-2 to DP-13, some up to DP-16; linear with hetero linkages: α1,4;1,6, ranging from DP-3 to DP-7 and β1,3;1,4 ranging from DP-3 to DP-16; branched with β1,3/β1,6 linkages, DP-2 to DP-13; and synthetic branched oligosaccharides with β1,3-linked linear DP-8 or DP-9 backbones, each with one or two β1,6-linked mono-glucosyl branches and a DP-4 backbone with an internal α1,3 linkage and two β1,6-linked glucose branches. Two xylo- and three manno-oligosaccharide NGLs were included as controls. Carbohydrate sequence information on these probes is in supplemental Table S7A. The binding signals are depicted as means of fluorescence intensities of duplicate spots at 5 fmol of oligosaccharide probe arrayed (with error bars) and are representative of at least two independent experiments; the numerical scores are given in supplemental Table S7B.
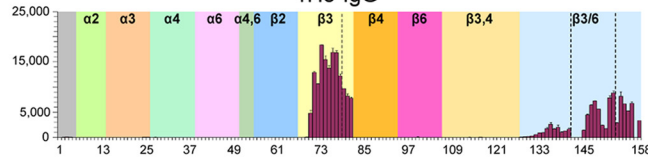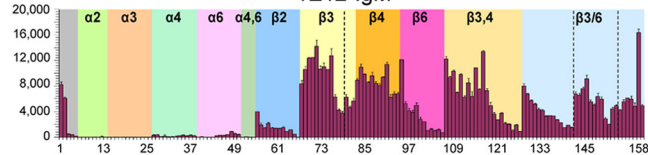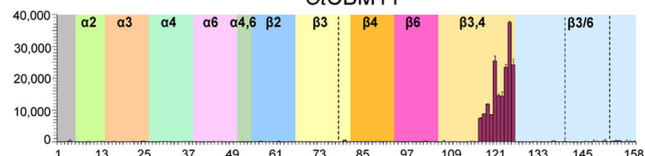
*Tm*CBM4–2, as predicted, showed selective binding to β1,3-gluco-oligosaccharides among linear sequences, similar to the binding by antibodies 2G8-IgG and 1H8-IgG, including the relatively weak binding to β1,3/6-branched oligosaccharides and the lack of binding to di-branched tetrasaccharide probe 157 (Fig. 5*B* and supplemental Tables S7A/B). Under

the microarray analysis conditions, a minimum chain length of DP-4 was required for binding.

For *Cm*CBM32–2, oligosaccharide ligands have not been described to our knowledge. In the microarray analyses, *Cm*CBM32–2 exhibited a similar binding profile to *Bh*CBM6 (Fig. 5*B*), the latter, as predicted, showed binding to the linear β1,3-gluco-oligosaccharides. On-array inhibition data confirmed binding of *Cm*CBM32–2 to short β1,3 oligosaccharides (supplemental Fig. S8). The two CBMs also showed prominent binding to linear β1,2-linked oligosaccharides and to β1,3/6-branched oligosaccharides. Binding could be detected to oligosaccharides as short as DP-2 or DP-3. Of note is the particularly strong binding of *Cm*CBM32–2 to the di-branched tetrasaccharide probe 157 compared with the unbranched β1,3-gluco-tetrasaccharide probe 68 (supplemental Tables S7A/B and supplemental Fig. S9), suggesting a possible involvement of the β1,6-branching in the recognition.

*Cm*CBM6–2 contains two binding clefts (A and B) that differ in specificity (supplemental Table S2). Binding was observed to linear β1,3- (attributable to cleft A), β1,4- (cleft A and B) and mixed β1,3/β1,4-linked oligosaccharides (cleft B) (Fig. 5*B*) that collectively would account for the higher binding intensities to a broader range of gluco-oligosaccharide probes than the preceding three CBMs. A novel finding was the robust binding to linear β1,2-gluco-oligosaccharides, which has not been reported for *Cm*CBM6–2. The binding to all of the β-linked gluco-oligosaccharides was detected at DP-2 and longer.

In sum, these antibodies and CBMs showed robust binding signals with differing binding patterns with respect to glucose linkage, sequence, and oligosaccharide chain length, not only agreeing with previous reports but also revealing novel specificities.

Application of the Glucome Microarray in Delineating Specificities of Two Signaling Molecules of the Immune System

Strict Specificity of Dectin-1—An unusual chain length requirement of Dectin-1 for binding to β1,3-linked linear gluco-oligosaccharides of DP-10 or greater was demonstrated in our earlier study in which only β1,3- and β1,6-linked linear oligosaccharide probes had been prepared. An important and frequently raised question remaining to be addressed was whether Dectin-1 can mediate signaling processes through interactions with other glucan sequences (45, 46). We now investigate here the range of gluco-oligosaccharide sequences bound by Dectin-1 using the glucome microarray.

Both the murine and human Dectin-1 behaved similarly (Fig. 6*A* and supplemental Fig. S7) and showed a highly restricted binding profile to the higher oligomers DP-11 to DP-13 of the linear β1,3-linked probes isolated from curdlan (probes 75–

77, supplemental Tables S7A/B). Binding was not detected to any other type of sequence nor to the other β1,3-containing oligosaccharides. Among the latter were chemically synthesized β1,3-linked oligosaccharides, DP-8 and DP-9, with one or two β1,6-linked mono-glucosyl branches (probes 152–156 and 158), or natural oligosaccharides isolated from branched polysaccharides containing β1,3 and β1,6-linkages up to DP-16, or those isolated from barley containing linear β1,3 and β1,4 linkages up to DP-16. The chain length requirement for Dectin-1 binding was corroborated by an "on-array" inhibition assay (supplemental Fig. S8).

Broad Binding Profile of DC-SIGN—The recognition of fuco- and manno-oligosaccharides by DC-SIGN has been thoroughly investigated. Information on the interactions of this protein with gluco-oligosaccharides is limited to inhibition of gp120 binding by gluco-disaccharides that are α1,4-, β1,4-, and β1,3-linked (47) and binding of DC-SIGN expressing cells to polyacrylamide neoglycoconjugates of gluco-disaccharide and tetrasaccharide that are α1,4-linked (8).

Microarray analyses of DC-SIGN showed a broad binding profile to gluco-oligosaccharides (Fig. 6*B*). There was strong binding to α1,4-linked probes with DP-2 and DP-3. This is in line with the reported interaction of DC-SIGN with *Mycobacterium tuberculosis,* through binding to its α-glucan, a capsular polysaccharide consisting predominantly of α1,4-linked glucose, which triggers the production of immunosuppressive IL-10 by activated DCs (8). Similarly to the α1,4-linked, all other gluco-oligosaccharide probes, DP-2 and DP-3 were preferentially bound by DC-SIGN. A novel finding in the present study is the prominent binding to β1,2-gluco-oligosaccharide probes: The DP-5 and DP-6 were particularly strongly bound, comparably to α1,4-linked glucose DP-2 and DP-3, β1,4-linked mannose DP-4 to DP-6 (Fig. 6*B*) and high-mannose *N*-glycans (not shown). There was also robust binding to the synthetic β1,3-linked gluco-tetrasaccharide with two β1,6-linked glucose branches and an internal α1,3 linkage (probe 157, supplemental Tables S7A/B).

These data highlight the contrasting behavior of these two signaling receptors among the proteins investigated (Fig. 6*B*): the long chain requirement and strict β1,3 specificity unique to Dectin-1 and preference for short chains but a broad range of glucose linkages/sequences for interaction with DC-SIGN.

DISCUSSION

Detailed assignments of binding specificities using intact glucan polysaccharides is hampered by the heterogeneous nature of the polysaccharides and difficulties in their separation/purification and unambiguous determination of glycan sequences they contain. Partial depolymerization to prepare gluco-oligosaccharides has been a conventional method for detailed investigation of structure/activity of glucans. At the oligosaccharide level, the difficulties in solubilizing the higher oligomers (*e.g.* DP > 7) is still a major problem to obtain sufficient amounts oligosaccharides of high purity for bioactivity and structural
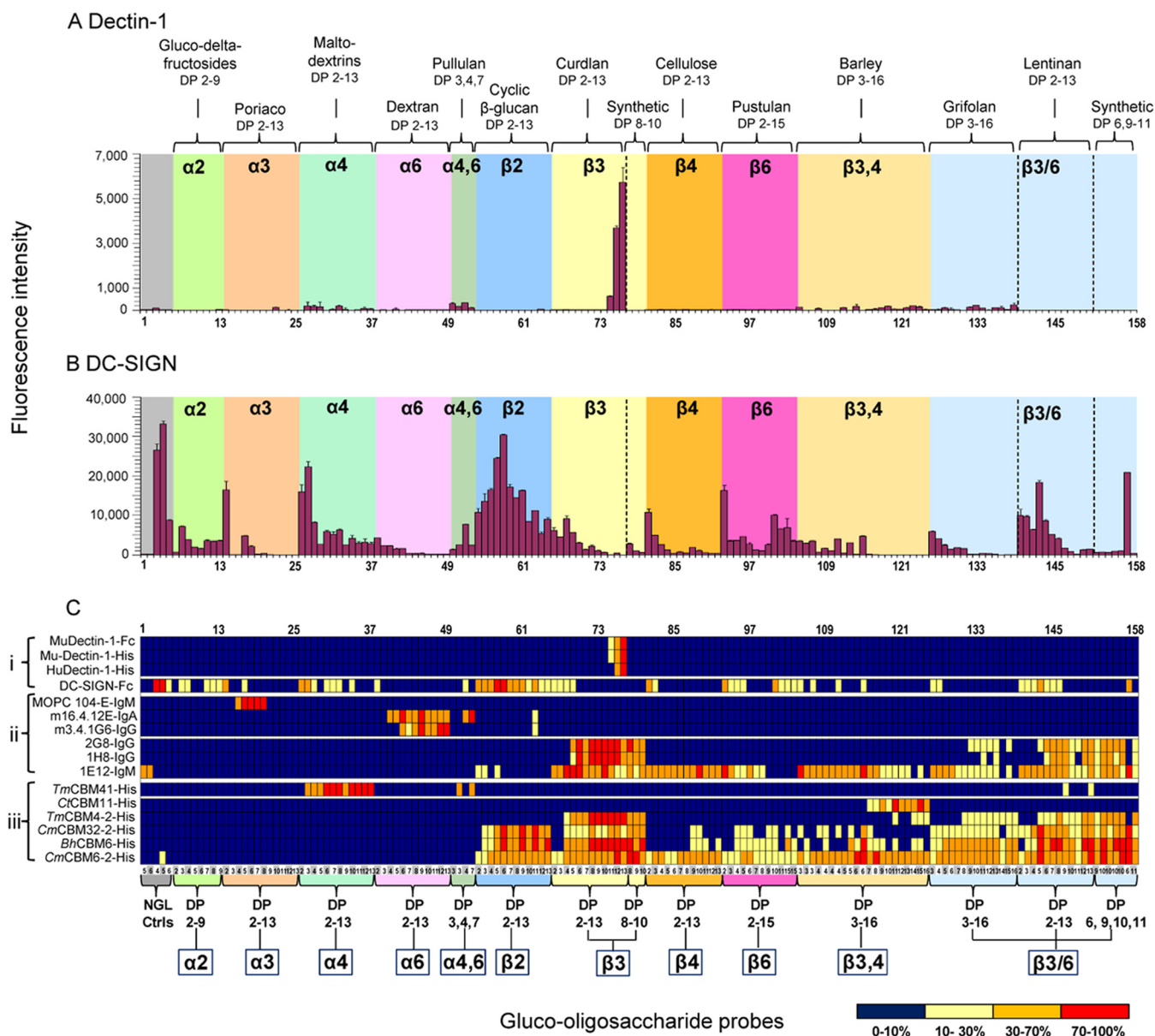
FIG. 6. **Application of the glucome-microarray to analyses of two signaling molecules of the immune system.** (*A*) Murine Dectin-1 and (*B*) human DC-SIGN analyzed as human Fc chimeras. (*C*) Comparison of the relative binding intensities of the three groups of proteins investigated: (i) mammalian lectin receptors of the immune system; (ii) monoclonal antibodies; and (iii) microbial CBMs. The heat map representation highlights the different glucan binding patterns revealed by the microarray analysis. The relative binding intensities were calculated as the percentage of the fluorescence signal intensity at 5 fmol given by the probe most strongly bound by each protein (normalized as 100%).

studies. In the approach we describe here, we address this by using a NGL-based microarray obtained from gluco-oligosaccharides prepared by fine-tuned depolymerization and fractionation/purification methods and the development of negative-ion ESI-CID-MS/MS for complete linkage and sequence analysis. Using multiple chromatographic means at microscale, we were able to obtain gluco-oligosaccharides of relatively high purity as demonstrated by validation with antibodies and other glucan-recognizing proteins of known specificities. Both the microarray and mass spectrometry are highly sensitive methods, and only very small amounts of oligosaccharides are required, thus en-

abling detection and unambiguous assignment of specificity of glucan recognition.

The partial fragmentation of the polysaccharides, the sequencing of the oligosaccharides by the negative-ion ESI-CID-MS/MS method, and their interrogation on the microarrays not only provide detailed information on linkage, sequence, and chain length requirements of glucan-recognizing proteins but also, as described here, are a sensitive means of revealing unsuspected sequences in the polysaccharides.

Glucan sequences recognized by the antibodies and CBMs that we selected as reference proteins had been determined

by independent methods such as inhibition of binding, ITC, x-ray crystallography, or STD-NMR. The prior knowledge served to validate the glucome microarray as a tool. At the same time, the wide range of gluco-oligosaccharide sequences covered in the microarrays has broadened knowledge on the specificities of *Bh*CBM6 and *Cm*CBM6–2, and revealed the ligands for antibody 1H8 and *Cm*CBM32–2 that had not been investigated previously.

Unlike Dectin-1, other glucan-recognizing proteins investigated, including CBMs with specificities for β1,3-linked glucose, did not have requirements for long chains and gave binding signals with oligosaccharides as short as DP-2 or DP-3 (Fig. 6*C*). The chain length requirements observed in the microarray analysis of these CBMs were correlated with the different modes of β1,3-glucan interaction in solution using STD-NMR (supplemental Fig. S10): CBMs that interact most strongly with the nonreducing end bind to short DP-2 or DP-3 sequences in the microarray, whereas those that interact with internal residues require longer chain lengths (supplemental Results).

Exquisite specificity of Dectin-1 for the linear β1,3-linkage is apparent in this glucome microarray. Reports using synthetic oligosaccharides as inhibitors (48, 49) of Dectin-1 binding are in accord with the chain-length requirement of Dectin-1 for *linear* β1,3-linked gluco-oligosaccharides. The β1,3/β1,6-branched oligosaccharides we examined were not bound by Dectin-1. These included those from lentinan and grifolan (analyzed up to DP-13 and DP-16, respectively) and the chemically synthesized oligosaccharides with β1,3-linked backbones of DP-8 and DP-9 with one or two β1,6-linked mono-glucosyl branches. In contrast, these branched oligosaccharides were bound by mAbs and CBMs that do not have such long-chain requirements (as depicted in supplemental Fig. S9). A possible explanation for lack of binding of Dectin-1 to the branched probes is their lack of a linear β1,3-linked backbone longer than DP-10, required by Dectin-1. We comment further on reported Dectin-1 inhibitory activities of certain branched oligosaccharides in supplemental Discussion and supplemental Table S8.

The glucome microarray has provided new insights into glucan recognition by DC-SIGN. The finding that β1,2-linked gluco-oligosaccharides are recognized by this signaling receptor is of potential functional significance, raising the possibility of interaction of DC-SIGN with *B. abortus* through recognition of its cyclic β1,2-glucan. Although the probes in the microarray were "linearized," this observation maybe an important clue to the involvement of DC-SIGN in the activation of dendritic cells by *B. abortus* cyclic β1,2-glucan (50). This requires exploration in depth.

In conclusion, we demonstrate the effectiveness and versatility of the glucome microarray for glucan recognition systems that require access to short as well as long gluco-oligosaccharide sequences with different linkages, sequences, and anomeric configurations. The microarray would be an effective tool for probing diverse other glucan recognition systems in fields including infection and immunity, also in functional analyses of proteins encoded by plant cell wall polysaccharide-degrading genes, while assisting the classification of newly identified CBMs or CBMs assigned to known families in the CAZy database. The present approach of designer microarrays coupled with MS opens the way to applying these approaches to the molecular dissection of immunostimulatory activities involving Dectin-1 where the presence of linear β1,3-sequences is not apparent (45, 46) and to assign carbohydrate recognition motifs involved in medicinal polysaccharide-driven immunostimulatory events (51).

*** To whom correspondence should be addressed: UCIBIO-REQUIMTE, Department of Chemistry, Faculty of Science and Technology, NOVA University of Lisbon, 2829-516 Caparica, Portugal. Tel: +351-21 294 8300(10940), E-mail: angelina.palma@fct.unl.pt. Glycosciences Laboratory, Department of Medicine, Imperial College London, London W12 0NN, UK. Tel: +44-20 7594 2596, E-mail: w.chai@imperial.ac.uk.

‡‡‡ Present address: Key Laboratory of Carbohydrate Chemistry and Biotechnology, Ministry of Education, School of Biotechnology, Jiangnan University, China.

§§§ Present address: College of Food Science and Technology, Huazhong Agricultural University, Wuhan, China.

REFERENCES

1. Brown, G. D., and Gordon, S. (2003) Fungal beta-glucans and mammalian immunity. *Immunity.* **19,** 311–315

2. Chen, J., and Seviour, R. (2007) Medicinal importance of fungal beta-(1−>3), (1−>6)-glucans. *Mycol. Res.* **111,** 635–652

3. Yamaguchi, T., Yamada, A., Hong, N., Ogawa, T., Ishii, T., and Shibuya, N. (2000) Differences in the recognition of glucan elicitor signals between rice and soybean: Beta-glucan fragments from the rice blast disease fungus *Pyricularia oryzae* that elicit phytoalexin biosynthesis in suspension-cultured rice cells. *Plant Cell* **12,** 817–826

4. Giavasis, I. (2014) Bioactive fungal polysaccharides as potential functional ingredients in food and nutraceuticals. *Curr. Opin. Biotechnol.* **26,** 162–173

5. Brown, G. D., Taylor, P. R., Reid, D. M., Willment, J. A., Williams, D. L., Martinez-Pomares, L., Wong, S. Y., and Gordon, S. (2002) Dectin-1 is a major beta-glucan receptor on macrophages. *J. Exp. Med.* **196,** 407–412

6. Chiani, P., Bromuro, C., Cassone, A., and Torosantucci, A. (2009) Anti-beta-glucan antibodies in healthy human subjects. *Vaccine* **27,** 513–519

7. Torosantucci, A., Chiani, P., Bromuro, C., De Bernardis, F., Palma, A. S., Liu, Y., Mignogna, G., Maras, B., Colone, M., Stringaro, A., Zamboni, S., Feizi, T., and Cassone, A. (2009) Protection by anti-beta-glucan antibodies is associated with restricted beta-1,3 glucan binding specificity and inhibition of fungal growth and adherence. *PLoS. ONE.* **4,** e5392

8. Geurtsen, J., Chedammi, S., Mesters, J., Cot, M., Driessen, N. N., Sambou, T., Kakutani, R., Ummels, R., Maaskant, J., Takata, H., Baba, O., Terashima, T., Bovin, N., Vandenbroucke-Grauls, C. M., Nigou, J., Puzo, G., Lemassu, A., Daffé, M., and Applmelk, B. J. (2009) Identification of mycobacterial alpha-glucan as a novel ligand for DC-SIGN: Involvement of mycobacterial capsular polysaccharides in host immune modulation. *J. Immunol.* **183,** 5221–5231

9. Gottar, M., Gobert, V., Matskevich, A. A., Reichhart, J. M., Wang, C., Butt, T. M., Belvin, M., Hoffmann, J. A., and Ferrandon, D. (2006) Dual detection of fungal infections in Drosophila via recognition of glucans and sensing of virulence factors. *Cell* **127,** 1425–1437

10. Arellano-Reynoso, B., Lapaque, N., Salcedo, S., Briones, G., Ciocchini, A. E., Ugalde, R., Moreno, E., Moriyón, I., and Gorvel, J. P. (2005) Cyclic [beta]-1,2-glucan is a brucella virulence factor required for intracellular survival. *Nat. Immunol.* **6,** 618–625

11. Gilbert, H. J., Knox, J. P., and Boraston, A. B. (2013) Advances in understanding the molecular basis of plant cell wall polysaccharide recognition by carbohydrate-binding modules. *Curr. Opin. Struct. Biol.* **23,** 669–677

12. Cuskin, F., Flint, J. E., Gloster, T. M., Morland, C., Baslé, A., Henrissat, B., Coutinho, P. M., Strazzulli, A., Solovyova, A. S., Davies, G. J., and Gilbert, H. J. (2012) How nature can exploit nonspecific catalytic and carbohydrate binding modules to create enzymatic specificity. *Proc. Natl. Acad. Sci. U.S.A.* **109,** 20889–20894

13. Hervé, C., Rogowski, A., Blake, A. W., Marcus, S. E., Gilbert, H. J., and Knox, J. P. (2010) Carbohydrate-binding modules promote the enzymatic deconstruction of intact plant cell walls by targeting and proximity effects. *Proc. Natl. Acad. Sci. U.S.A.* **107,** 15293–15298

14. Fontes, C. M., and Gilbert, H. J. (2010) Cellulosomes: highly efficient nanomachines designed to deconstruct plant cell wall complex carbohydrates. *Annu. Rev. Biochem.* **79,** 655–681

15. Zhang, M., Chekan, J. R., Dodd, D., Hong, P. Y., Radlinski, L., Revindran, V., Nair, S. K., Mackie, R. I., and Cann, I. (2014) Xylan utilization in human gut commensal bacteria is orchestrated by unique modular organization of polysaccharide-degrading enzymes. *Proc. Natl. Acad. Sci. U.S.A.* **111,** 3708–3717

16. van Bueren, A. L., Higgins, M., Wang, D., Burke, R. D., and Boraston, A. B. (2007) Identification and structural basis of binding to host lung glycogen by streptococcal virulence factors. *Nat. Struct. Mol. Biol.* **14,** 76–84

17. Wang, J., Stuckey, J. A., Wishart, M. J., and Dixon, J. E. (2002) A unique carbohydrate binding domain targets the lafora disease phosphatase to glycogen. *J. Biol. Chem.* **277,** 2377–2380

18. Fukui, S., Feizi, T., Galustian, C., Lawson, A. M., and Chai, W. (2002) Oligosaccharide microarrays for high-throughput detection and specificity assignments of carbohydrate-protein interactions. *Nat. Biotechnol.* **20,** 1011–1017

19. Rillahan, C. D., and Paulson, J. C. (2011) Glycan microarrays for decoding the glycome. *Annu. Rev. Biochem.* **80,** 797–823

20. Song, X., Lasanajak, Y., Xia, B., Heimburg-Molinaro, J., Rhea, J. M., Ju, H., Zhao, C., Molinaro, R. J., Cummings, R. D., and Smith, D. F. (2011) Shotgun glycomics: A microarray strategy for functional glycomics. *Nat. Methods* **8,** 85–90

21. Pedersen, H. L., Fangel, J. U., McCleary, B., Ruzanski, C., Rydahl, M. G., Ralet, M. C., Farkas, V., von, Schantz, L., Marcus, S. E., Andersen, M. C., Field, R., Ohlin, M., Knox, J. P., Clausen, M. H., and Willats, W. G. (2012) Versatile high resolution oligosaccharide microarrays for plant glycobiology and cell wall research. *J. Biol. Chem.* **287,** 39429–39438

22. Palma, A. S., Feizi, T., Childs, R. A., Chai, W., and Liu, Y. (2014) The neoglycolipid (NGL)-based oligosaccharide microarray system poised to decipher the meta-glycome. *Curr. Opin. Chem. Biol.* **18,** 87–94

23. Feizi, T., and Chai, W. (2004) Oligosaccharide microarrays to decipher the glyco code. *Nat. Rev. Mol. Cell Biol.* **5,** 582–588

24. Palma, A. S., Feizi, T., Zhang, Y., Stoll, M. S., Lawson, A. M., Diaz-Rodríguez, E., Campanero-Rhodes, M. A., Costa, J., Gordon, S., Brown, G. D., and Chai, W. (2006) Ligands for the beta-glucan receptor, Dectin-1, assigned using 'designer' microarrays of oligosaccharide probes (neoglycolipids) generated from glucan polysaccharides. *J. Biol. Chem.* **281,** 5771–5779

25. Ashline, D. J., Yu, Y., Lasanajak, Y., Song, X., Hu, L., Ramani, S., Prasad, V., Estes, M. K., Cummings, R. D., Smith, D. F., and Reinhold V. N. (2014) Structural characterization by multistage mass spectrometry (MSn) of human milk glycans recognized by human rotaviruses. *Mol. Cell. Proteomics.* **13,** 2961–2974

26. Yu, Y., Mishra, S., Song, X., Lasanajak, Y., Bradley, K. C., Tappert, M. M., Air, G. M., Steinhauer, D. A., Halder, S., Cotmore, S., Tattersall, P., Agbandje-McKenna, M., Cummins, R. D., and Smith, D. F. (2012) Functional glycomic analysis of human milk glycans reveals the presence of virus receptors and embryonic stem cell biomarkers. *J. Biol. Chem.* **287,** 44784–44799

27. Yu, Y., Lasanajak, Y., Song, X., Hu, L., Ramani, S., Mickum, M. L., Ashline, D. J., Prasad, B. V., Estes, M. K., Reinhold, V. N., Cummings, R. D., and Smith, D. F. (2014) Human milk contains novel glycans that are potential decoy receptors for neonatal rotaviruses. *Mol. Cell Proteomics.* **13,** 2944–2960

28. Dell, A., and Morris, H. R. (2001) Glycoprotein structure determination by mass spectrometry. *Science* **291,** 2351–2356

29. König, S., and Leary, J. A. (1998) Evidence for linkage position determination in cobalt coordinated pentasaccharides using ion trap mass spectrometry. *J Am. Soc. Mass Spectrom.* **9,** 1125–1134

30. Tseng, K., Hedrick, J. L., and Lebrilla, C. B. (1999) Catalog-library approach for the rapid and sensitive structural elucidation of oligosaccharides. *Anal. Chem.* **71,** 3747–3754

31. Wheeler, S. F., and Harvey, D. J. (2000) Negative ion mass spectrometry of sialylated carbohydrates: Discrimination of N-acetylneuraminic acid linkages by MALDI-TOF and ESI-TOF mass spectrometry. *Anal. Chem.* **72,** 5027–5039

32. Zaia, J., McClellan, J. E., and Costello, C. E. (2001) Tandem mass spectrometric determination of the 4S/6S sulfation sequence in chondroitin sulfate oligosaccharides. *Anal. Chem.* **73,** 6030–6039

33. Pfenninger, A., Karas, M., Finke, B., and Stahl, B. (2002) Structural analysis of underivatized neutral human milk oligosaccharides in the negative ion mode by nano-electrospray MSn (Part 2: Application to isomeric mixtures). *J. Am. Soc. Mass Spectrom.* **13,** 1341–1348

34. Chai, W., Piskarev, V., and Lawson, A. M. (2001) Negative-ion electrospray mass spectrometry of neutral underivatized oligosaccharides. *Anal. Chem.* **73,** 651–657

35. Zhang, H., Zhang, S., Tao, G., Zhang, Y., Mulloy, B., Zhan, X., and Chai, W. (2013) Typing of blood-group antigens on neutral oligosaccharides by negative-ion electrospray ionization tandem mass spectrometry. *Anal. Chem.* **85,** 5940–5949

36. Chai, W., Piskarev, V., and Lawson, A. M. (2002) Branching pattern and sequence analysis of underivatized oligosaccharides by combined MS/MS of singly and doubly charged molecular ions in negative-ion electrospray mass spectrometry. *J. Am. Soc. Mass Spectrom.* **13,** 670–679

37. Maina, N. H., Juvonen, M., Domingues, R. M., Virkki, L., Jokela, J., and Tenkanen, M. (2013) Structural analysis of linear mixed-linkage glucooligosaccharides by tandem mass spectrometry. *Food Chemistry* **136,** 1496–1507

38. Fischer, D., Loos, E., and Geyer, A. (2006) Oligo-(1−>2)-alpha-D-glucopyranosyl-(1−>2)-beta-D-fructofuranosides Form Tight Sugar Coils. *Angewandte Chemie International Edition* **45,** 816–819

39. Liu, Y., Feizi, T., Campanero-Rhodes, M. A., Childs, R. A., Zhang, Y.,

Mulloy, B., Evans, P. G., Osborn, H. M., Otto, D., Crocker, P. R., and Chai, W. (2007) Neoglycolipid probes prepared via oxime ligation for microarray analysis of oligosaccharide-protein interactions. *Chem. Biol.* **14,** 847–859

40. Chai, W., Stoll, M. S., Galustian, C., Lawson, A. M., and Feizi, T. (2003) Neoglycolipid technology—Deciphering information content of glycome. *Methods Enzymol.* **362,** 160–195

41. Liu, Y., Childs, R. A., Palma, A. S., Campanero-Rhodes, M. A., Stoll, M. S., Chai, W., and Feizi, T. (2012) Neoglycolipid-based oligosaccharide microarray system: Preparation of NGLs and their noncovalent immobilization on nitrocellulose-coated glass slides for microarray analyses. *Methods Mol. Biol.* **808,** 117–136

42. Stoll, M. S., and Feizi, T. (2009). Software tools for storing, processing and displaying carbohydrate microarray data. Proceeding of the Beilstein Symposium on Glyco-Bioinformatics, 4–8 October, 2009, Potsdam, Germany. (ed. C. Kettner), pp. 123–140. Beilstein Institute for the Advancement of Chemical Sciences, Frankfurt, Germany.

43. Domon, B., and Costello, C. E. (1988) A systematic nomenclature for carbohydrate fragmentations in FAB-MS/MS spectra of glycoconjugates. *Glycoconjugate J.* **5,** 397–409

44. Huang, Q., and Zhang, L. (2005) Solution properties of (1–>3)-alpha-D-glucan and its sulfated derivative from Poria cocos mycelia via fermentation tank. *Biopolymers* **79,** 28–38

45. Rothfuchs, A. G., Bafica, A., Feng, C. G., Egen, J. G., Williams, D. L., Brown, G. D., and Sher, A. (2007) Dectin-1 interaction with Mycobacterium tuberculosis leads to enhanced IL-12p40 production by splenic dendritic cells. *J. Immunol.* **179,** 3463–3471

46. Tada, R., Ikeda, F., Aoki, K., Yoshikawa, M., Kato, Y., Adachi, Y., Tanioka, A., Ishibashi, K., Tsubaki, K., and Ohno, N. (2009) Barley-derived beta-D-glucan induces immunostimulation via a dectin-1-mediated pathway. *Immunol. Lett.* **123,** 144–148

47. Su, S. V., Hong, P., Baik, S., Negrete, O. A., Gurney, K. B., and Lee, B. (2004) DC-SIGN binds to HIV-1 glycoprotein 120 in a distinct but overlapping fashion compared with ICAM-2 and ICAM-3. *J. Biol. Chem.* **279,** 19122–19132

48. Adams, E. L., Rice, P. J., Graves, B., Ensley, H. E., Yu, H., Brown, G. D., Gordon, S., Monteiro, M. A., Papp-Szabo, E., Lowman, D. W., Power, T. D., Wempe, M. F., and Williams, D. L. (2008) Differential high-affinity interaction of dectin-1 with natural or synthetic glucans is dependent upon primary structure and is influenced by polymer chain length and side-chain branching. *J. Pharmacol. Exp. Ther.* **325,** 115–123

49. Tanaka, H., Kawai, T., Adachi, Y., Hanashima, S., Yamaguchi, Y., Ohno, N., and Takahashi, T. (2012) Synthesis of beta(1,3) oligoglucans exhibiting a Dectin-1 binding affinity and their biological evaluation. *Bioorg. Med. Chem.* **20,** 3898–3914

50. Martirosyan, A., Perez-Gutierrez, C., Banchereau, R., Dutartre, H., Lecine, P., Dullaers, M., Mello, M., Salcedo, S. P., Muller, A., Leserman, L., Levy, Y., Zurawski, G., Zurawski, S., Gorvel, J-P. (2012). Brucella beta 1,2 cyclic glucan is an activator of human and mouse dendritic cells. *PLoS Patholog.* **8,** e1002983

51. Hsu, T. L., Cheng, S. C., Yang, W. B., Chin, S. W., Chen, B. H., Huang, M. T., Hsieh, S. L., and Wong, C. H. (2009) Profiling carbohydrate-receptor interaction with recombinant innate immunity receptor-Fc fusion proteins. *J. Biol. Chem.* **284,** 34479–34489